Journal of Medicinal Chemistry

Article

pubs.acs.org/jmc

Synthesis, Aqueous Reactivity, and Biological Evaluation of Carboxylic Acid Ester-Functionalized Platinum–Acridine Hybrid Anticancer Agents

Leigh A. Graham,[†] Jimmy Suryadi,[†] Tiffany K. West,[‡] Gregory L. Kucera,[‡] and Ulrich Bierbach*,[†]

[†]Department of Chemistry, Wake Forest University, Winston-Salem, North Carolina 27109, United States

[‡]Department of Internal Medicine, Section on Hematology and Oncology, Wake Forest University Health Sciences, Winston-Salem, North Carolina 27157, United States

Supporting Information

ABSTRACT: The synthesis of platinum–acridine hybrid agents containing carboxylic acid ester groups is described. The most active derivatives and the unmodified parent compounds showed up to 6-fold higher activity in ovarian cancer (OVCAR-3) and breast cancer (MCF-7, MDA-MB-231) cell lines than cisplatin. Inhibition of cell proliferation at nanomolar concentrations was observed in pancreatic (PANC-1) and nonsmall cell lung cancer cells (NSCLC, NCI-H460) of 80- and 150-fold, respectively. Introduction of the ester groups did not affect the cytotoxic properties of the hybrids, which form the same monofunctional–intercalative DNA adducts as the parent compounds, as demonstrated in a plasmid unwinding assay. In-line high-performance liquid chromatography and electrospray mass spectrometry (LC-ESMS) shows that the ester moieties undergo platinum-mediated hydrolysis in a chloride concentration-dependent manner to form carboxylate chelates. Potential applications of the chloride-sensitive ester hydrolysis as a self-immolative release mechanism for tumor-selective delivery of platinum–acridines are discussed.

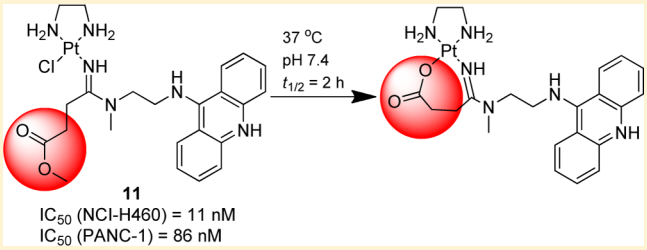

INTRODUCTION

The clinical utility of the DNA cross-linking agent cisplatin (**1**) (Chart 1) as a life-prolonging chemotherapeutic agent is limited by various mechanisms of acquired tumor resistance and the drug's narrow spectrum of activity.[1,2] Most cancers are inherently resistant to platinum-based therapies, and curative effects are observed only in germ cell tumors.[3] For instance, in nonsmall cell lung cancer (NSCLC), a major cause of cancer mortality in both men and women, platinum is used as a palliative treatment without a major survival advantage.[4] Recent insight into the genetics of NSCLC resistance to cisplatin suggests that this drug is largely ineffective because the DNA adducts it forms are removed by nucleotide excision repair (NER), which is upregulated in this type of aggressive cancer.[5−7] Among the novel cytotoxics developed to combat this and other forms of chemoresistant cancers, nonclassical platinum drugs mechanistically distinct from cisplatin have demonstrated unique clinical potential because of their ability to overcome resistance at the nuclear level and induce cancer cell death by alternative mechanisms.[8,9]

Chart 1

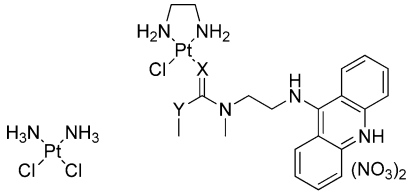

Platinum–acridine agents derived from the prototypical agent [PtCl(en)(1-[2-(acridin-9-ylamino)ethyl]-1,3-dimethylthiourea)]$(NO_3)_2$ (PT-ACRAMTU) (Chart 1), which form monofunctional–intercalative DNA adducts but do not cross-link DNA, have shown excellent activity in solid tumors resistant to cisplatin, in particular NSCLC cell lines.[10] Specifically, compound **3** (Chart 1), generated by replacement of the thiourea in **2** (PT-ACRAMTU) with an amidine donor and related derivatives, have demonstrated a cytotoxic enhancement relative to cisplatin of up to 500-fold in NSCLC cell lines.[11,12] Compound **3** produces significantly higher intracellular concentrations and DNA adduct levels in NCI-H460 cells than cisplatin,[13] and the hybrid adduct itself proves to be a significantly more severe form of DNA damage than the common bifunctional cross-link.[14] The cumulative effect of these pharmacological parameters renders the hybrid agent an efficient inhibitor of DNA replication and inducer of cell death.[15]

While the second-generation platinum–acridines show potent cytotoxic properties that translate into promising

Received: June 22, 2012
Published: August 7, 2012

tumor inhibition in vivo, the dose-limiting toxicity observed in test animals suggests that modifications of these agents are necessary to improve their pharmacological properties.[12] Specifically, we are interested in introducing platinum–acridines as cytotoxic "warheads" in receptor-targeted therapies or as payloads attached to tumor-directed carriers using chemically or enzymatically reversible linkers. To achieve this goal, modification of the original structures with conjugatable functional groups is necessary. This is not a trivial task, as many modifications made to cytotoxics, for instance to deliver them as a payload reversibly attached to monoclonal antibodies, have been shown to diminish the agent's biological activity.[16] Here, we have investigated the chemical and biological effects of attaching a carboxylic acid ester group to the nonleaving acridine moiety in compound **3**. We demonstrate that the ester-modified hybrid agents, which maintain high activity in various solid tumor cell lines, are excellent models of caged carboxylato-functionalized hybrids. On the basis of the aqueous reactivity of these molecules, a novel self-immolative mechanism of drug activation/release via platinum-catalyzed chloride concentration-sensitive ester hydrolysis to free carboxylate is proposed.

RESULTS

Design and Synthesis. The design of the ester-modified platinum–acridines reported here was inspired by previous attempts to reduce the reactivity of these agents in circulation by exchanging the chloro leaving group in compound **3** with sterically hindered monocarboxylato ligands.[11] These ligands proved to be extremely labile, which resulted in undesired intramolecular substitution of the oxygen donor by the 9-amino group of the acridine moiety to produce a substitution-inert, marginally cytotoxic nitrogen chelate. We reasoned that incorporation of the carboxylato ligand as a pendant group into a chelate, similar to the dicarboxylato leaving group in the clinical drug carboplatin,[1] should produce a more stable, yet DNA reactive entity. Thus, initially the synthetic goal of this study was to generate a suitable precursor molecule by installing a carboxylic acid ester group at the amidine moiety of the acridine carrier ligand that can be converted into a carboxylate chelate (Scheme 1). Precedent for this reaction was found in analogous Pt(II) and Pd(II) complexes containing ester-substituted pyridine ligands.[17]

Scheme 1. Proposed Conversion of Ester Precursor to Chelated Carboxylato Ligand

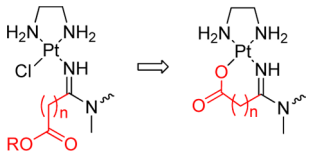

The desired target compounds in this study were synthesized using methodology developed for compound **3** and related analogues, which involves highly efficient addition of a suitably modified 9-aminoacridine derivative across the activated CN triple bond in the appropriate platinum–nitrile complexes to produce an amidine linkage.[11,12] Three ester-modified hybrids (compounds **10**–**12**) and, for comparison, two simple propionamidine derivatives (**3′** and **9**), were synthesized and isolated as mononitrate salts (Scheme 2) (note: compound **3′** is the +1 charged form of compound **3**). While compounds **3′**, **9**, **11**, and **12** were isolated in >85% yield and >95% analytical purity, the synthesis of derivative **10** suffered from an inherent instability of precursor complex **5** (decarboxylation, dimerization) as a consequence of the reactivity of the methylcyanoacetate ligand (see Supporting Information). From the reaction mixtures, we were able to isolate milligram quantities of compound **10** using semipreparative reverse-phase HPLC (see Supporting Information) sufficient for cytotoxicity assays in one of the more sensitive cell lines.

Scheme 2. Synthesis of Target Compounds[a]

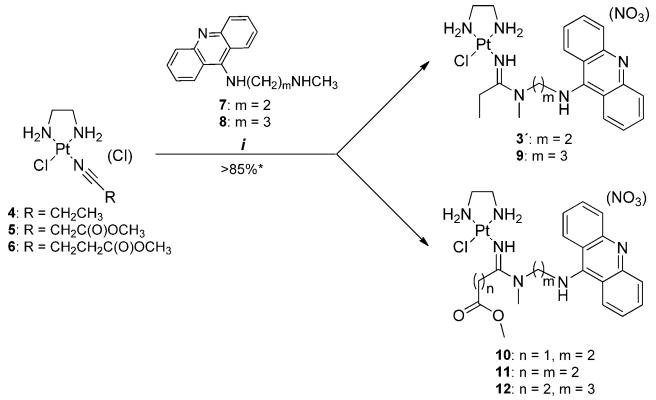

[a]Reagents and conditions: (*i*) (1) $AgNO_3$, DMF, rt (anion exchange), (2) **7** or **8**, DMF, −10 °C, 2 h, (3) MeOH, Et_2O. * For **3′**, **9**, **11**, and **12**. Only a few milligrams of pure compound **10** were isolated.

Biological Activity. The newly synthesized platinum–acridines were studied along with cisplatin in NSCLC (NCI-H460), ovarian (OVCAR-3), breast (MDA-MB-231, MCF-7), and pancreatic (PANC-1) cancer cell lines using a colorimetric cell proliferation assay. The results are summarized in Table 1. The majority of the platinum–acridines screened performed significantly better than cisplatin in all cancer cell lines in this assay based on the inhibitory concentrations calculated from the drug–response curves. While the most active analogues in each series showed a 3–6-fold enhanced cytotoxicity compared to the clinical drug in the ovarian and breast cancer cell lines, a dramatic increase in cytotoxic potency of approximately 80-fold and 150-fold was observed in the pancreatic and NSCLC cell line, respectively. Cisplatin inhibits cell proliferation at micromolar concentrations, as typically observed for this drug in solid tumor cell lines.[18] By contrast, several of the simple (**3′** and **9**) and ester-modified (**10**–**12**) platinum–acridines show effective cell kill in the nanomolar concentration range.

In addition to these global trends in activity and chemosensitivity, two important structure–activity relationship features emerge in the set of compounds tested. First, extension of the propionamidine moieties in compounds **3′** and **9** with a methyl ester group, giving derivatives **11** and **12**, did not have a negative effect on the cytotoxicity of the hybrids, except in the case of the pair **9**/**12** in OVCAR-3, where the activity of the ester-modified compound decreases by approximately 5-fold. In most cases, compounds **11** and **12** exhibited cytotoxicities similar to those of their unmodified counterparts. This was unexpected because it has previously been observed that addition of steric bulk in this part of the molecule results in a decrease in cytotoxicity.[11] Another critical trend observed across the entire data set is that the hybrids in which the platinum moiety is separated from the intercalator by an extended propylene linker (m = 3 in **9** and **12**) show greatly

dx.doi.org/10.1021/jm300879k | J. Med. Chem. 2012, 55, 7817–7827

Table 1. Summary of Cytotoxicity Data for Platinum−Acridines and Cisplatin in Human Solid Tumor Cell Lines

	IC_{50} (μM) ± SEM[a]				
compd	NCI-H460	OVCAR-3	MDA-MB-231	MCF-7	PANC-1
cisplatin (**1**)	1.2 ± 0.2	3.3 ± 0.4	60 ± 7	12 ± 2	6.6 ± 0.7
3′ (m = 2)[b]	0.008 ± 0.002	1.1 ± 0.1	15 ± 2	2.5 ± 0.1	0.09 ± 0.01
9 (m = 3)	0.052 ± 0.006	33 ± 9	37 ± 5	11 ± 1	4.4 ± 0.6
10 (n = 1, m = 2)	0.036 ± 0.006	*c*	*c*	*c*	*c*
11 (n = m = 2)	0.011 ± 0.001	1.9 ± 0.4	9.9 ± 1.4	3.6 ± 0.3	0.086 ± 0.009
12 (n = 2, m = 3)	0.065 ± 0.008	150 ± 40	36 ± 2	19 ± 1	2.2 ± 0.6

[a]Concentrations of compound that reduce cell viability by 50%, determined in 72 h drug incubations using a colorimetric cell proliferation assay. Values are means of three independent experiments performed in triplicate ± the standard error of the mean. [b]For definitions of n and m, see Scheme 2. [c]Tested only in NCI-H460 due to insufficient material (see text).

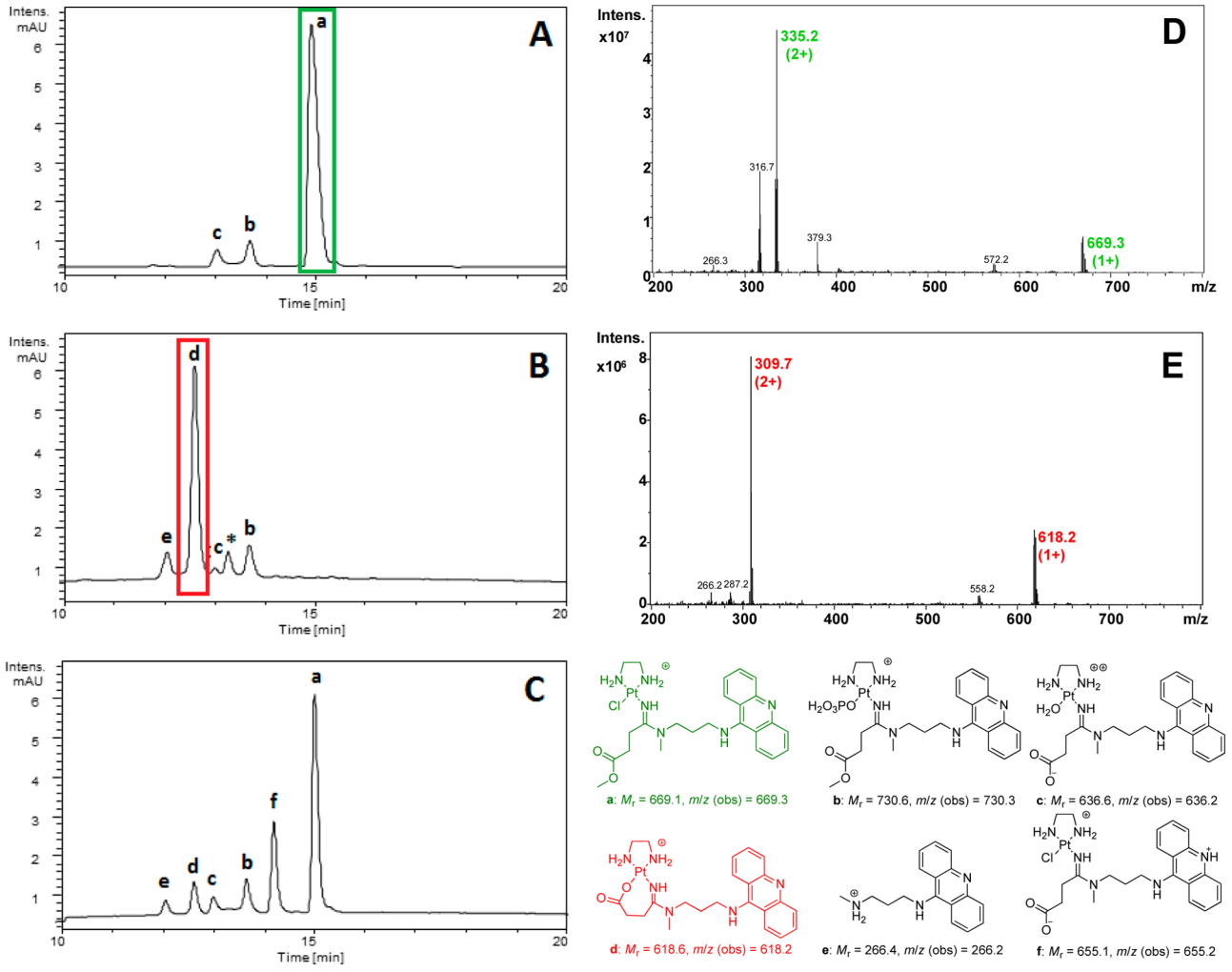

Figure 1. Reverse-phase HPLC analysis of a 1 mM solution of complex **12** in (A) 10 mM phosphate buffer (pH 7.4) prior to incubation, (B) 10 mM phosphate buffer after 18 h of incubation at 37 °C, and (C) 10 mM phosphate buffer containing 150 mM NaCl after 18 h of incubation at 37 °C. HPLC traces were recorded with a monitoring wavelength range of 363−463 nm specific for the acridine chromophore. Structures of the species assigned to peaks a−f are shown in the lower right-hand panel. The asterisk in (B) denotes an unidentified product. (D) Electrospray mass spectrum recorded in positive-ion mode of intact compound **12** (HPLC fraction a). Characteristic ions: m/z 669.3 ($[M]^+$), 335.2 ($[M]^{2+}$), 116.7 ($[M - Cl]^{2+}$). (E) Electrospray mass spectrum recorded in positive-ion mode of the carboxylate chelate (HPLC fraction d). Characteristic ions: m/z 618.2 ($[M]^+$), 309.7 ($[M]^{2+}$).

reduced cell kill potential. For instance, in NCI-H460, derivatives **3′** and **11** (with m = 2) are approximately six times more cytotoxic than compounds **9** and **12**. This effect is even more pronounced in the cell lines OVCAR-3 and PANC-1. Compound **10** (n = 1, m = 2), which was tested only in NCI-H460 cells, was 3−4 times less cytotoxic than compounds **3′** and **11**. In other words, extension of the amidine side chain by one methylene group (n = 2 in **11** vs n = 1 in **10**) significantly improves the cell kill activity in this particular cell line.

Aqueous Reactivity. Compounds **10**−**12** were designed as potential prodrugs of the respective carboxylato complexes and as model compounds to test the utility of carboxylic acid esters

dx.doi.org/10.1021/jm300879k | J. Med. Chem. 2012, 55, 7817−7827

as cleavable groups in cancer-cell or tumor-tissue targeted conjugates. Attempts to synthesize the corresponding closed carboxylato chelate complexes (Scheme 1) from compounds **10**–**12** were unsuccessful and were abandoned after it was established that these form spontaneously on a physiologically relevant time scale in pH neutral solution, as described below.

To study the aqueous chemical reactivity of the pendant ester functional groups under physiologically relevant conditions, compounds **11** and **12** were incubated at 37 °C in phosphate buffer (pH 7.4) and in phosphate buffer supplemented with 150 mM NaCl. The latter media was chosen to simulate chloride concentrations in circulation. The reaction mixtures were then analyzed at various time points by in-line high-performance liquid chromatography–electrospray mass spectrometry (LC–ESMS). Complexes **11** and **12** were found to show the same reactivity, which was expected because the only difference between the two analogues is an extended acridine linkage (m = 2 in **11** vs m = 3 in **12**). Because the reaction mixtures produced by compound **12** resulted in superior chromatographic (baseline) separations, results were analyzed in detail and will be discussed for this derivative. Selected analytical data (for mass spectra of all species, see Supporting Information) and structures of the species identified in the mixtures are summarized in Figure 1.

When a freshly prepared sample of compound **12** in 10 mM phosphate buffer was analyzed, the HPLC trace showed 90% chemically unchanged **12** (Figure 1A), based on the molecular ion and fragment ions observed in mass spectra recorded in positive-ion mode (Figure 1D). Additionally, two minor products were identified, consistent with substitution of the chloro ligand in **12** by phosphate (peak b, Figure 1A), as well as an aquated form that has undergone ester hydrolysis (peak c, Figure 1A). After 18 h of incubation at 37 °C, complete conversion of compound **12** was observed. The major species detected in the corresponding HPLC trace (peak d, Figure 1B), which accounts for 70% of the product mixture, is easily identified as the proposed carboxylate chelate in which the chloro ligand has been replaced with carboxylate oxygen (Figure 1E). In addition, small amounts (<10%) of nonchelated species and acridine–amine **8** were observed (peak e), the latter product suggesting minor degradation of the hybrid (~10%), which was unexpected. When incubations were performed under the same conditions in a buffer containing 150 mM NaCl, approximately 55% of compound **12** remained in the mixture chemically unchanged (Figure 1C), and the carboxylate chelate shows an abundance of only 17%. Under these high-chloride conditions, 22% of the hydrolyzed ester product exists in the form of the chloro complex containing a dangling carboxylate (peak f, Figure 1C). This observation is consistent with facile opening of the seven-membered N,O chelate by this relatively weak donor.

The incubations in buffer mimicking biological media show that the efficiency of ester hydrolysis in compound **12** is reduced by high chloride concentrations, which suggests that cleavage of the ester group is mediated to a significant extent by platinum. To gain insight into the kinetics of ester cleavage in the presence and absence of chloride ion, the time course of ester conversion was monitored by LC–ESMS. This was possible by integrating the peaks in the chromatograms recorded for samples withdrawn from the reaction mixtures at various time points during the first 6 h of incubation. The percentage of the total platinum species present in solution in which the ester moiety was converted to chelated or dangling carboxylate (fractions c, d, and f, see Figure 1) was then plotted against reaction time (Figure 2). From curve fits of the data

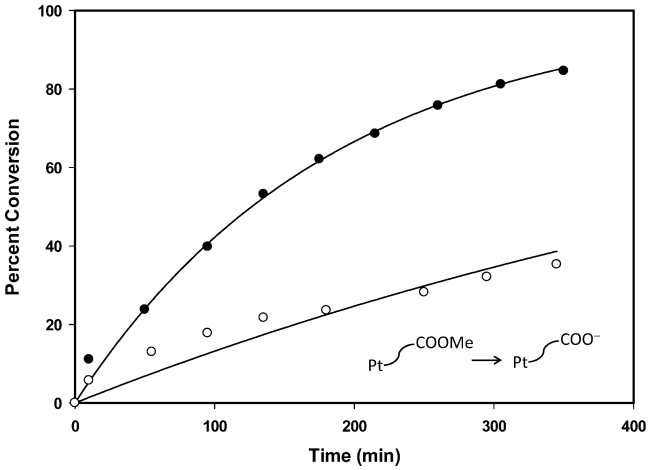

Figure 2. Time course of ester hydrolysis in compound **12** at 37 °C monitored by quantitative HPLC in phosphate-buffered (pH 7.4) solution (●) and in 10 mM phosphate buffer containing 150 mM NaCl (○). Species in solution were quantified by integrating HPLC traces recorded over a wavelength range of 363–463 nm specific for the acridine chromophore. The lines represent curve fits to the equation $y = a\ (1 - e^{bx})$, where a is the extrapolated maximum conversion and $b = k$ (s^{-1}). The experiment was performed in duplicate with similar results.

assuming first-order reaction kinetics, half-lives of 2 and 8 h were estimated for ester hydrolysis in chloride-free and chloride-containing media, respectively. Incubations of compound **12** in chloride-free acidic solution in the pH range 1–5 (adjusted with HNO_3) did not lead to significant cleavage of the ester group. By contrast, rapid ester hydrolysis is observed at pH > 9. Under these conditions, relative larger amounts of compound **12** decompose to produce free acridine–amine **8** (data not shown).

On the basis of the pH and chloride concentration dependence of ester hydrolysis observed in complex **12**, an intramolecular, metal-mediated mechanism is proposed in which platinum acts as a catalytic Lewis acid (Scheme 3). Ester cleavage may proceed either via internal attack of an

Scheme 3. Proposed Mechanism of Platinum-Catalyzed Ester Hydrolysis

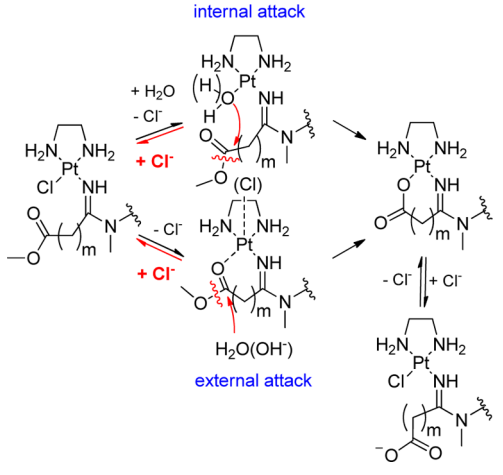

dx.doi.org/10.1021/jm300879k | J. Med. Chem. 2012, 55, 7817–7827

activated aqua (hydroxo) ligand or via external attack of the metal activated ester group by water or hydroxide ion. Both pathways of the proposed mechanism, which are in complete analogy to the platinum-catalyzed intramolecular hydrolysis observed for peptide bonds,[19] would explain why suppression of (reversible) aquation of the complex by high concentrations of external chloride inhibits ester hydrolysis catalyzed by platinum.

Reactivity with DNA Nitrogen and Amino Acid Sulfur. To study the effect of the pendant ester groups and the corresponding carboxylato chelates in the platinum−acridines in reactions with DNA nitrogen, compound **11** was incubated with excess 5′-guanosine monophosphate (5′-GMP, disodium salt). The reactions were performed with complex **11** in phosphate-buffered solution prior to and after complete hydrolysis of the ester and monitored by quantitative LC−ESMS analysis. For comparison, incubations were also performed with compound **3′** under the same conditions. Quantitative HPLC analysis shows that compound **3′** converts nearly quantitatively to monofunctional adduct with a half-life of 80 min (Figure 3). By contrast, the analogous reactions with

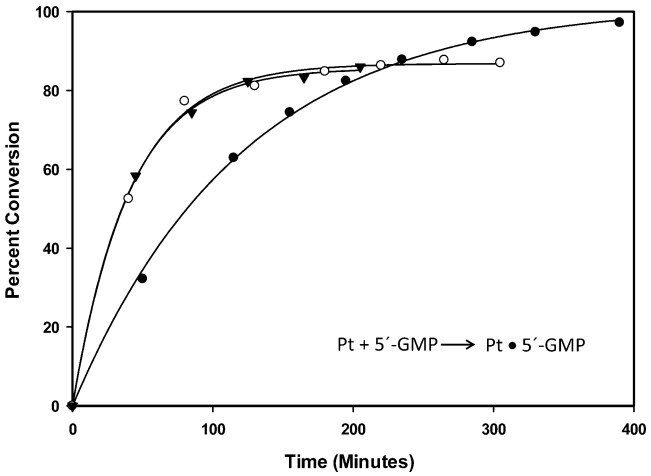

Figure 3. Time course of adduct formation with 5′-GMP at 37 °C (1 mM Pt, 10 mM nucleotide) for compound **11** (triangles), the carboxylate chelate formed from compound **11** after 18 h of preincubation in phosphate buffer (○), and compound **3′** (●) monitored by quantitative HPLC in phosphate-buffered (pH 7.4) solution. Nucleotide adduct in solution was identified by recording mass spectra in positive-ion mode and quantified by integrating HPLC traces recorded over a wavelength range of 363−463 nm. The lines represent curve fits to the equation $y = a\ (1 - e^{bx})$, where a is the extrapolated maximum conversion and $b = k\ (s^{-1})$. Experiments were performed in duplicate with similar results.

intact compound **11** and its hydrolyzed form do not go to completion but show approximately 85% conversion, which may be a result of the above-noted partial decomposition of the compound. However, both species react with the mononucleotide significantly faster than compound **3′** with a half-life of less than 30 min. Formation of monofunctional adducts in all three cases was confirmed by electrospray mass spectrometry (Figure 4A). While the high reactivity of the seven-membered carboxylato chelate can be expected because oxygen is a better leaving group than chloride, the fact that compound **11** reacts faster than compound **3′** with guanine nitrogen despite the added steric bulk of the ester functional group is surprising. One possible explanation for this rate enhancement might be that the ester group acts as an internal auxiliary nucleophile that enhances nucleotide binding by catalyzing the rate-limiting loss of chloride (see *external pathway* in Scheme 3). In reactions of **11** with 5′-GMP, nucleotide binding outcompetes ester hydrolysis, resulting in modification of the nucleotide mainly with the intact ester derivative (adduct II in Figure 4A) rather than the hydrolyzed form, of which only traces are observed (adduct III in Figure 4A).

The reactivity of the three platinum−acridines with glutathione (GSH) was also studied using the same experimental setup. Incubations of the platinum complexes with one equivalent of GSH at 25 °C resulted in stoichiometric replacement of the leaving group with the tripeptide to produce adducts of a 1:1 stoichiometry (Figure 4B). Reactions with the sulfur nucleophile proceeded rapidly in all cases, making it impossible to determine half-lives chromatographically (and by proton NMR spectroscopy). An important outcome of this assay is that the carboxylate chelate in the hydrolysis product does not seem to protect platinum from nucleophilic attack by GSH sulfur, a reaction that has been implicated as a cause of tumor resistance and nephrotoxicity of cisplatin.[20] The high reactivity with sulfur was expected based on the facile substitution of coordinated carboxylate by chloride observed in the high-salt phosphate buffer.

DNA Interactions. Introduction of an ester functionality in compounds **3′** (giving **11**) and **9** (giving **12**) did not have a major impact on the cytotoxic potency of the agents (Table 1). On the other hand, extension of the alkylene linker connecting platinum to the acridine intercalator in this set of compounds by only one carbon atom (e.g., $m = 2$ in **3′** vs $m = 3$ in **9**) resulted in a pronounced decrease in cytotoxicity. To assess if the effects observed in cells may be mediated at the DNA adduct level, a plasmid unwinding assay was performed. This assay has been used routinely to determine the local untwisting of closed-circular supercoiled DNA induced by different types of platinum−DNA adducts,[21] including those produced by platinum−acridines.[22,23] The unwinding produced per adduct extracted from these experiments provides insight into the binding mode of a DNA-modifying agent. In this experiment, negatively supercoiled pUC19 plasmid was modified with compounds **3′**, **9**, and **11** at varying platinum-to-DNA nucleotide ratios (r_b) and analyzed by gel electrophoresis (Figure 5). The results show that the hybrid adduct formed by the prototypical agent **3′** unwinds the duplex by 17 ± 1°. This value is in excellent agreement with the unwinding produced by compound **3** in site-specifically modified model duplexes.[14] Furthermore, the data demonstrate that compounds **9** and **11** produce essentially the same degree of unwinding as the parent compound (16 ± 1°), suggesting that extension of the linker by one methylene group or addition of a dangling ester group have no effect on the intercalation geometry in the hybrid adducts. Quantitation of platinum bound to the DNA samples after 24 h of incubation and subsequent removal of unbound agent by microdialysis shows that only ∼64% of compound **11** forms permanent adducts with the plasmid, whereas binding of the parent compound **3′** is quantitative under the same conditions (see Supporting Information). The reduced binding levels observed for compound **11** may be caused by partial conversion of the ester into a carboxylate chelate and the electrostatically unfavorable negative charge introduced into the DNA adducts by the carboxylate. However, despite being a less efficient inducer of hybrid adducts in this assay, compound **11** appears to cause the same distortions in DNA per adduct as compound

dx.doi.org/10.1021/jm300879k | J. Med. Chem. 2012, 55, 7817−7827

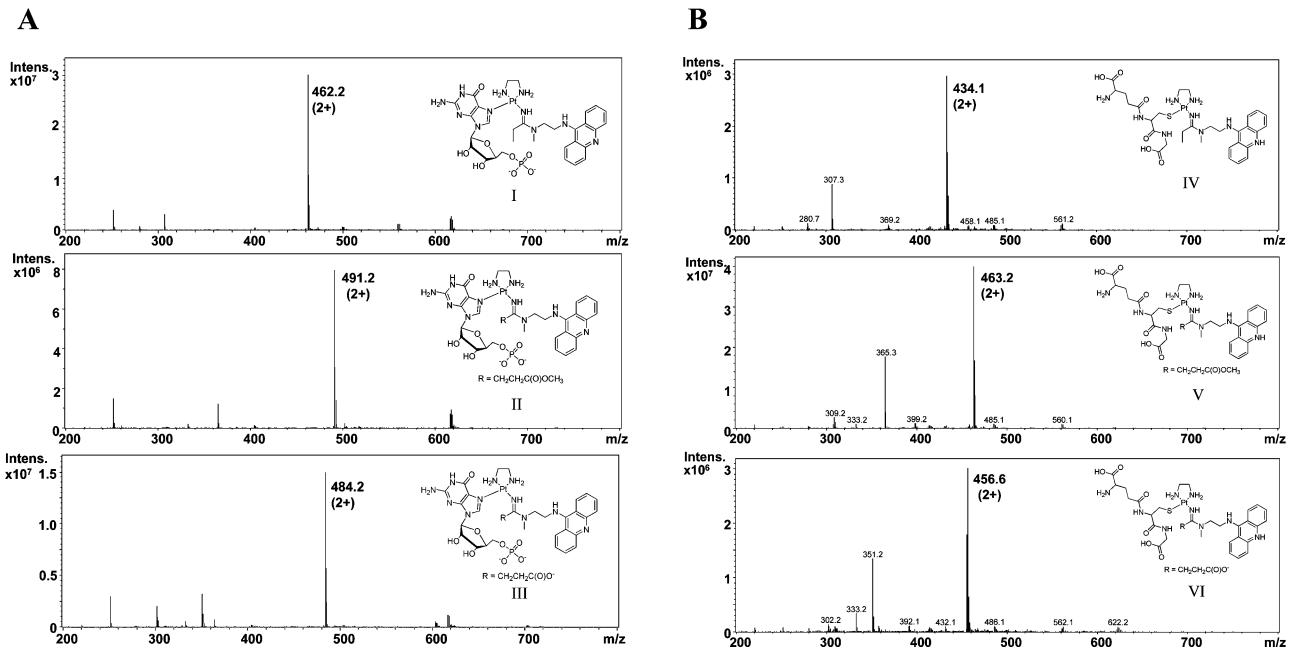

Figure 4. Electrospray mass spectra recorded in positive-ion mode in the 200−800 m/z range of adducts formed in reactions of platinum−acridines **3′**, **11**, and hydrolyzed **11** with (A) 5′-GMP and (B) GSH in phosphate-buffered solution at 37 and 25 °C, respectively. All molecular ions are observed in their 2+ charged form.

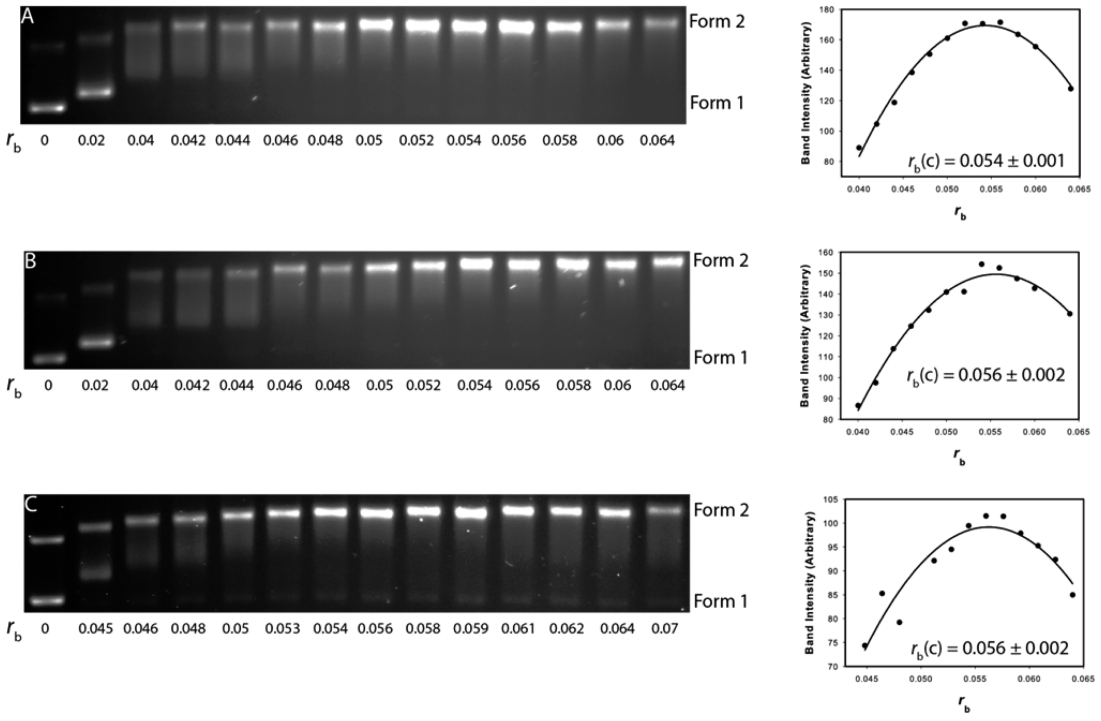

Figure 5. DNA unwinding study of pUC19 plasmid modified with varying amounts ($0.02 < r_b < 0.07$) of compounds **3′** (A), **9** (B), and **11** (C). Ethidium stained agarose gels are shown along with quadratic polynomial fits of integrated band intensities around the coalescence points. The $r_b(c)$ is the platinum-to-nucleotide ratio at which the supercoiled plasmid (form 1) has been completely converted into open-circular, relaxed plasmid (form 2 showing the highest band intensity). The unwinding angles (ϕ) calculated were 17 ± 1° for compound **3′** and 16 ± 1° for compounds **9** and **11** (see Experimental Section for details).

3′. Because of the inherent hydrolytic reactivity of compound **11**, the plasmid reacted with it likely contains adducts featuring dangling ester and carboxylate groups. In that case, the observed unwinding angle would suggest that both adducts produce similar structural effects in DNA. To study the effect of a dangling anionic carboxylate group on the DNA binding mode, unwinding experiments were also performed with prehydrolyzed compound **11** (not shown). Because ester hydrolysis leads to product mixtures of varying composition depending on the buffer system used, unwinding experiments performed with the reaction mixtures gave inconsistent results and were not pursued further.

dx.doi.org/10.1021/jm300879k | J. Med. Chem. 2012, 55, 7817−7827

The differences in cancer cell kill observed for compounds **3′** and **9** are unlikely a consequence of differences in the DNA adducts they form, as both analogues produce the same DNA helical perturbations. However, while both compounds show the same mode of intercalation, extension of the linker from *m* = 2 (in **3′**) to *m* = 3 (in **9**) may have an effect on the *rate* with which platinum binds with nucleobase nitrogen. This is a possibility because increasing the spacing between acridine and platinum may affect the nucleophilic attack of nucleobase nitrogen on the metal at the site of intercalation. To investigate the time course of platination of DNA by derivatives **3′** and **9**, we took advantage of the compounds' ability to efficiently convert negatively supercoiled DNA (form 1) into the fully relaxed form (form 2). Because only irreversibly bound platinum–acridine contributes to the unwinding of plasmid DNA in this assay,[22] the rate at which the relaxed (open-circular) form is generated is directly proportional to the rate of platination.

In this experiment, pUC19 plasmid was incubated at the same concentration of platinum that produces adduct levels high enough to completely convert form 1 of the DNA into form 2 ($r_i \approx 0.07$, see Figure 5). Samples were withdrawn from the incubation mixtures at various time points and quenched with excess thiourea under conditions where the sulfur nucleophile binds to platinum to prevent further reaction with DNA but does not reverse existing DNA adducts.[24] Samples were then analyzed by agarose gel electrophoresis to determine the relative rates of formation of form 2 of the plasmid. A comparison of the two electrophoretic separations (Figure 6A,B) clearly shows that derivative **9** produces form 2 at a significantly slower rate than derivative **3′**. This qualitative assessment is based on the relatively lower intensity of the corresponding band on the gel observed for the former derivative and the fact that partially relaxed topoisomers (diffuse bands of intermediate mobility) persist longer for **9** than for **3′**. A plot of integrated band intensities vs reaction time for form 2 of the plasmid generated by **3′** and **9** confirms this observation (Figure 6C). From curve fits of the data to first-order reaction kinetics, half-lives of 43 and 77 min were estimated for **3′** and **9**, respectively (Figure 6C). In conclusion, while the acridine chromophores in the two derivatives appear to produce similar intercalation geometries in the final DNA adducts they form, extending the linker by one methylene group leads to less efficient platination of nucleobase nitrogen. This decrease in DNA reactivity may contribute to the loss in cytotoxic potency observed for compound **9**.

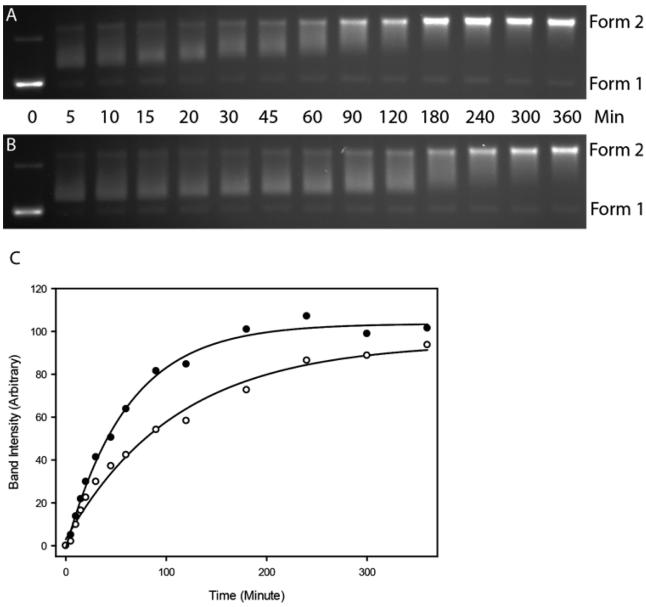

Figure 6. Kinetics of unwinding of pUC19 plasmid by platinum–acridines studied by electrophoretic analysis for compounds **3′** (A) and **9** (B). Electrophoretic separations in (A) and (B) were run on the same agarose gel to minimize artifacts due to inconsistent ethidium staining and integration of the bands. (C) Plot of integrated band intensities for form 2 of the plasmid vs time for compounds **3′** (●) and **9** (○). The data was fitted to the single exponential equation $y = C + a(1 - e^{-bt})$, where b is the apparent first-order rate constant of the binding processes, k_{app}. For compound **3′**, $k_{app} = 2.7 \times 10^{-4}$ s^{-1} and $t_{1/2}$ = 43 min, compound **9** $k_{app} = 1.5 \times 10^{-4}$ s^{-1} and $t_{1/2}$ = 77 min.

DISCUSSION

In a search for targeted prodrug technologies for the delivery of highly cytotoxic platinum–acridine hybrid agents, we have evaluated the utility of carboxylic acid ester-modified derivatives. We demonstrated that addition of suitable 9-aminoacridine precursors to platinum-bound (functionalized) nitrile is a suitable synthetic strategy for incorporating an ester group into the carrier side chain of these hybrid agents. Platinum–nitrile complexes, such as compound **6**, prove to be versatile synthons for generating structurally and functionally diverse hybrid agents. The clean and high-yield conversion to hybrid agent in the absence of byproduct, which are the hallmarks of organic click chemistry,[25] has been used here to generate compounds **11** and **12**. The synthetic scheme, however, proved to be impractical for generating compound **10** due to the inherent instability of precursor complex **5**. This limitation complicates the synthesis of carboxylate-modified hybrid agents of sufficient purity and stability able to form potentially less reactive six-membered carboxylate chelates (such as compound **10**).

The biological consequences of introducing an ester group into the hybrid agents and structure–activity relationships in this set of compounds were studied in five solid tumor cell lines. NCI-H460, which represents an aggressive form of lung cancer, has been shown to be most responsive to platinum–acridine treatment and was included in this assay as a benchmark. The fact that compound **11** maintains nanomolar activity in this cell line correlates well with the DNA interactions established for the compound and supports previous observations, implying that nanomolar activity in this type of cancer requires rapid formation of hybrid adducts in cellular DNA.[13,24] The approximately six times lower cytotoxicity observed for compound **9** compared to **3′** (the same trend is observed for the pair **11**/**12**) suggests that DNA-binding efficiency is directly correlated with cytotoxicity in this rapidly proliferating cancer. However, it cannot be ruled out that subtle differences in compound uptake or in the structures and recognition of their DNA adducts may also contribute to the differences in biological activity.

OVCAR-3 is a cell line derived from an ovarian tumor refractory to cisplatin. The level of resistance observed in these cells is closely correlated with high levels of GSH,[26] and we reasoned that the proposed intracellular formation of the carboxylate chelates from the ester precursors might protect platinum from detoxification by the sulfur-containing tripeptide. Overall, compounds **3′** and **11** show slightly better activity in this cell line than cisplatin. The fact that the ester derivatives

dx.doi.org/10.1021/jm300879k | J. Med. Chem. 2012, 55, 7817–7827

had no advantage over the unmodified parent compounds, however, suggests that the conversion of compounds **11** and **12** into carboxylate chelates plays no role as a protective mechanism. While intracellular conversion to the chelated form can be expected during the 72 h incubations of the cancer cells with platinum (based on the $t_{1/2}$ of 2 h of chelate formation in buffered neutral solution, see Figure 2), we also demonstrated that this form of the agent would readily react with GSH.

Significantly higher cytotoxicity was observed for the most potent platinum–acridines than for cisplatin in the breast cancer lines MCF-7 and MDA-MB-231, which were included in this panel because they are generally insensitive to chemotherapy.[27] Especially in hormone-dependent breast cancers, such as estrogen receptor-positive MCF-7, platinum–acridines may have applications as a cytotoxic component in combination therapies or multifunctional targeted therapies (see Discussion). Finally, PANC-1 was included in this panel. Screening in this pancreatic cancer cell line was inspired by the compelling mechanistic similarities between the drug gemcitabine (Gemzar), one of the most effective therapies in pancreatic cancer,[28] and platinum–acridine **3**. Unlike cisplatin, both agents are very efficient inhibitors of DNA synthesis and induce cell-cycle arrest in late G1/early S phase.[15,29] Compounds **3′** and **11** are highly cytotoxic at submicromolar concentrations in PANC-1, whereas micromolar concentrations of cisplatin (Table 1) and gemcitabine[28] are required to produce the same cell kill effect in this cell line. Given these promising results, platinum–acridines will be studied as systemic and targetable cytotoxics in additional pancreatic cancer models.

The high reactivity of the seven-membered carboxylate chelate precludes the use of compound **11** as a simple nontargeted prodrug to help overcome GSH-mediated tumor resistance and/or reduce systemic toxicity. The ester technology however provides a unique opportunity for tuning the biodistribution of the platinum–acridines and for delivering them to target tissues. This should be possible by attaching the hybrid agents to suitable carrier systems using cleavable ester linkages. Potential delivery vehicles include, for instance, polymeric and nanosized materials and small molecules that bind to cancer cell-specific receptors. Simple lipophilic groups, such as fatty acid esters and glycerides in place of the simple methyl ester in compound **11**, would be an interesting option to tune the hydrophilic/lipophilic balance and enhance the passive permeability of the hybrids. The ideal conjugates would be sufficiently stable in circulation where the high chloride concentration should suppress complex aquation and metal-promoted ester cleavage. Once internalized into the cancer cell, hydrolysis of the ester linkage is triggered by the low chloride concentration in the cytosol, resulting in the self-immolative release[30] of hybrid agent (Figure 7). To achieve this design goal, additional structural modifications may be necessary that extend the half-life of the ester group, which may also be prone to spontaneous and enzymatic cleavage in plasma. In essence, this approach will exploit the classical mechanism of activation of platinum drugs by intracellular complex aquation[31] for the targeted release of platinum–acridines.

CONCLUSION

In conclusion, in this study an ester-functionalized form of the platinum–acridine pharmacophore was generated and studied as a cytotoxic agent in various cancer models. The modified agent shows the same high cell-kill potential as the unmodified parent compound, which translates into promising submicromolar activity in NSCLC NCI-H460 and previously untested pancreatic PANC-1. The high sensitivity of the latter cell line to the hybrid agents is exciting given the urgent need for novel treatment options to tackle pancreatic cancer. Efficient targeting of this and other types of cancer investigated in this study using appropriate carrier molecules in conjunction with novel self-immolative release mechanisms may improve the toxicity profile and in vivo efficacy of the platinum–acridines.

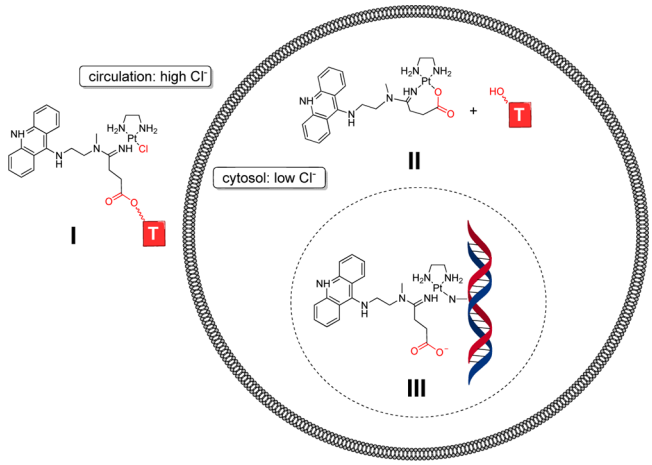

Figure 7. Proposed mechanism of action of tumor-targeted platinum–acridines based on ester cleavage triggered in a chloride concentration gradient. (I) Passive accumulation in tumor tissue or active targeting of cancer cell by an ester-linked tumor-selective carrier molecule (targeting moiety, shown as rectangular red box labeled "T"). (II) Self-immolative release of cytotoxic agent triggered by complex aquation. (III) Formation of cytotoxic DNA adducts in cell nucleus.

EXPERIMENTAL SECTION

Materials and Procedures. Cisplatin (**1**), 5′-guanosine monophosphate (5′-GMP, disodium salt, 99%), and glutathione (reduced form, 98–100%) were purchased from Sigma. The platinum precursor $[PtCl_2(en)]$ (en = ethane-1,2-diamine) was synthesized by the method of Dhara.[32] Compounds **3′**, **4**, **7**, and **8** were synthesized previously.[11,12,33,34] For the preparation of biological buffers, biochemical grade chemicals (Fisher/Acros) were used. HPLC-grade solvents were used for all HPLC and mass spectrometry experiments. All reagents were used as obtained without further purification.

^{1}H NMR spectra of the target compounds and intermediates were recorded on Bruker Advance 300 and DRX-500 instruments operating at 300 and 500 MHz, respectively. $^{13}C\{^1H\}$ NMR spectra were recorded on a Bruker DRX-500 instrument operating 125.8 MHz. Chemical shifts (δ) are given in parts per million (ppm) relative to tetramethylsilane (TMS). Electrospray mass spectra were recorded on an Agilent 1100LC/MSD ion trap mass spectrometer. Ion evaporation was assisted by a flow of N_2 drying gas (300–350 °C) at a pressure of 40–50 psi and a flow rate of 11 L/min. Mass spectra were typically recorded with a capillary voltage of 2800 V and a mass-to-charge (m/z) scan range of 200–2200. The purity of the target compounds and the composition of reactions mixtures was analyzed by reverse-phase high-performance liquid chromatography (HPLC) using the LC module of an Agilent Technologies 1100 LC/MSD trap system equipped with a multiwavelength diode-array detector. Separations were performed on a 4.6 mm ×150 mm reverse-phase Agilent ZORBAX SB-C18 (5 μm) analytical column at 25 °C. The following solvent system was used: solvent A, optima water, and solvent B, methanol/0.1% formic acid, at a flow rate of 0.5 mL/min and a gradient of 95% A to 5% A over 25 min. HPLC traces were recorded over a wavelength range of 363–463 nm. Peak integration was

dx.doi.org/10.1021/jm300879k | J. Med. Chem. 2012, 55, 7817–7827

accomplished with the LC/MSD Trap Control 4.0 data analysis software. For target compounds studied in cancer cells and DNA binding experiments, an analytical purity of ≥95% was confirmed using this setup.

[PtCl(en)($C_4H_5NO_2$)]Cl (5). The complex [$PtCl_2$(en)] (300 mg, 1.23 mmol) was heated under reflux in DI H_2O (5 mL) with methyl cyanoacetate (5 mL, excess) until the yellow suspension turned into a colorless solution (∼1 h). Solvent was removed by rotary evaporation. The pale-yellow residue was dried in a vacuum at 40 °C and dissolved in 5 mL of dry methanol. The solution was passed through a syringe filter, and the colorless filtrate was added directly into 150 mL of vigorously stirred dry diethyl ether. The resulting white precipitate was isolated by membrane filtration and dried in a vacuum, yielding complex **5** as an off-white microcrystalline solid, which was filtered off and dried in a vacuum. Yield: 207 mg of a moisture-sensitive crude product, which could not be further purified but used directly for the synthesis of compound **10** (see Supporting Information for details of the product characterization by LC-MS).

[PtCl(en)($C_5H_7NO_2$)]Cl (6). This analogue was prepared as described for **5** starting from 200 mg (0.613 mmol) and methyl cyanopropionate (2 mL, excess) in 3 mL of DI H_2O. Yield: 183 mg (68%). ^{1}H NMR (MeOH-d_4) δ 5.93 (4H, m), 3.75 (3H, s), 3.18 (2H, t, J = 6.6 Hz), 2.82 (2H, t, J = 6.6 Hz), 2.59 (4H, m). ESMS (+ve mode): m/z 403.0 ([M]$^+$).

[PtCl(en)($C_{20}H_{24}N_4$)]NO_3 (9). Platinum–nitrile complex **4** (200 mg, 0.526 mmol) was converted to its nitrate salt by reaction with $AgNO_3$ (85 mg, 0.500 mmol) in 4 mL of anhydrous DMF. AgCl was removed by syringe filtration, and the filtrate was cooled to −10 °C. *N*-(Acridin-9-yl)-*N*′-methylpropane-1,3-diamine (**8**) (140 mg, 0.524 mmol) was added, and the suspension was stirred at −10 °C until it turned into a deep-orange solution (∼2 h). After treatment with activated carbon, the reaction mixture was filtered through a Celite pad and added dropwise into 200 mL of vigorously stirred diethyl ether. The yellow slurry was stirred for ∼30 min. The bright-yellow precipitate was recovered by membrane filtration, washed exhaustively with dry diethyl ether to remove excess acridine–amine **8**, and dried in a vacuum at 60 °C overnight. Yield 286 mg (85%). ^{1}H NMR (MeOD-d_4) δ 8.31 (2H, d, J = 8.1 Hz), 7.82 (2H, d, J = 8.7 Hz), 7.69 (2H, t, J = 7.7 Hz), 7.39 (2H, t, J = 7.7 Hz), 3.95 (2H, t, J = 6.8 Hz), 3.40 (2H, t, J = 7.5 Hz), 2.85 (5H, overl. m), 2.55 (4H, m), 2.03 (2H, p, J = 7.4 Hz), 1.17 (3H, t, J = 7.1 Hz). ^{13}C{^{1}H} NMR (MeOH-d_4) δ 171.1, 155.2, 147.7, 132.6, 132.4, 129.2, 126.7, 125.6, 123.9, 117.2, 66.9, 28.9, 15.5, 11.7. ESMS (+ve mode): m/z 611.2 ([M]$^+$), 305.7 ([M + H]$^{2+}$), 575.2 (M − Cl − H]$^+$, 287.2 (M − Cl]$^{2+}$).

[PtCl(en)($C_{20}H_{22}N_4O_2$)]NO_3 (10). This derivative was prepared analogously to compound **9**. Starting from complex **5** (450 mg, 1.06 mmol) and acridine–amine **7** (258 mg, 1.03 mmol), 489 mg of crude product were obtained, which contained major amounts of impurities that could not be removed by recrystallization (see text and Supporting Information). An analytically pure sample of complex **10** was generated by HPLC purification on a Hitachi D-7000 HPLC system equipped with a L-7420 UV–vis detector using a 9.4 mm × 250 mm reverse-phase Agilent ZORBAX SB-C18 (5 μm) semi-preparative column. The following solvent system was used: solvent A, optima water, and solvent B, methanol/0.1% formic acid, with a flow rate of 0.75 mL/min and a gradient of 95% A to 5% A over 45 min. A monitoring wavelength of 413 nm was used to identify acridine-containing products. Approximately 10 mg of compound **10** of 95% purity were generated. ESMS (+ve mode): m/z 641.2 ([M]$^+$), 321.1 ([M + H]$^{2+}$), 302.7 (M − Cl]$^{2+}$).

[PtCl(en)($C_{21}H_{24}N_4O_2$)]NO_3 (11). This derivative was prepared analogously to compound **9**. Starting from complex **6** (300 mg, 0.684 mmol) and acridine–amine **7** (170 mg, 0.676 mmol), 419 mg (86%) of compound **11** were obtained. ^{1}H NMR (MeOH-d_4) δ 8.28 (2H, d, J = 8.5 Hz), 7.70 (4H, overl. m), 7.25 (2H, t, J = 7.5 Hz), 4.11 (2H, t, J = 6.3), 3.79 (2H, t, J = 6.3 Hz), 3.68 (3H, s), 3.29 (2H, t, J = 8.3 Hz), 2.60 (3H, br. s), 2.93 (2H, t, J = 6.3 Hz), 2.59 (4H, overl. m). ^{13}C{^{1}H} NMR (MeOH-d_4) δ 172.7, 168.1, 154.2, 131.3, 125.2, 124.7, 122.4, 65.5, 30.3, 29.3, 14.1. ESMS (+ve mode): m/z 655.1 ([M]$^+$), 328.0 ([M + H]$^{2+}$), 309.2 (M − Cl]$^{2+}$).

[PtCl(en)($C_{22}H_{26}N_4O_2$)]NO_3 (12). This derivative was prepared analogously to compound **9**. Starting from 310 mg (0.708 mmol) of complex **6** and 187 mg (0.705 mmol) of acridine–amine **8**, 459 mg (89%) of compound **12** were obtained. ^{1}H NMR (MeOD-d_4) δ 8.31 (2H, d, J = 8.5 Hz), 7.80 (2H, d, J = 8.5 Hz), 7.69 (2H, t, J = 7.3 Hz), 7.38 (2H, t, J = 7.3 Hz), 3.94 (2H, t, J = 7.0 Hz), 3.65 (3H, s), 3.46 (2H, t, J = 7.3 Hz), 3.21 (2H, t, J = 8.0 Hz), 2.96 (3H, s), 2.90 (2H, t, J = 8.3 Hz), 2.53 (4H, m), 2.06 (2H, p, J = 7.3 Hz). ^{13}C{^{1}H} NMR (MeOD-d_4) δ 174.1, 168.8, 155.1, 147.6, 132.4, 125.6, 123.8, 117.3, 52.4, 49.931.7, 30.5, 29.4. ESMS (+ve mode): m/z 668.2 ([M]$^+$), 335.1 ([M + H]$^{2+}$), 316.2 (M − Cl]$^{2+}$).

Incubations. Ester hydrolysis in compounds **11** and **12** was studied by incubating the respective agent (1 mM) in a 10 mM phosphate buffer (pH 7.4, with and without 150 mM NaCl) at 37 °C for 18 h. The reaction mixtures were analyzed by in-line LC-MS using the experimental setup described under Materials and Procedures. All reaction mixtures were diluted with methanol/formic acid to a final concentration of platinum of 20 μM immediately prior to injection into the LC unit. To study the kinetics of chelate formation, the same reactions were carried out, however, LC-MS spectra were collected of samples withdrawn from the incubation mixtures and quenched on ice approximately every 45 min over a period of 6 h. Reactions with 5′-guanosine monophosphate (5′-GMP) and glutathione (GSH) were performed at a 1:10 drug-to-nucleophile ratio in the same (NaCl-free) phosphate buffer. (The same conditions were applied for samples of **11** and **12** that were preincubated in chloride-free phosphate buffer at 37 °C for 18 h). Incubations with nucleophiles were performed at 37 °C for 24 h. The reaction mixtures were analyzed by LC-MS as described in the previous section. Time-dependent data were fitted to (pseudo) first-order reaction kinetics using SigmaPlot (version 12.0, Systat Software, San Jose, CA).

DNA Unwinding Assay. Plasmid DNA (pUC19, 2686 bp) was generated by transforming a chemically competent *Escherichia coli* (NovaBlue, Novagen) with pUC19 and extracted from the cells using Qiagen's MegaPrep Plasmid kit (Qiagen, Valencia, CA). Plasmid concentrations were determined spectrophotometrically at 260 nm with ε = 6500 $M^{-1}\cdot cm^{-1}$ (nucleotides, n.t.). To modify the DNA with known amounts of platinum agent, pUC19 plasmid (5 μM n.t.) was incubated in TE buffer (10 mM Tris/1 mM EDTA, pH 7.5) overnight at 37 °C with **3′**, **9**, and **11** at various platinum-to-nucleotide ratios (r_i) (r_i = 0.01–0.2; for accurate determination of the coalescence point, r_b(c), the range of modification was narrowed down to r_i = 0.02–0.07). Incubation concentrations of the platinum hybrid agents were determined from their absorbances at 413 nm in water using an extinction coefficient of 10^5 $M^{-1}\cdot cm^{-1}$.[12,22] The progress of DNA adduct formation for **3′** and **9** was monitored at various time points (5–360 min) by quenching samples with 7 μM thiourea and chilling at 0 °C. Bound platinum-to-nucleotide ratios (r_b) around the coalescent points were determined by inductively coupled plasma mass spectrometry (ICP-MS) using a previously reported protocol.[13] Samples were dialyzed against 8 L of Milli-Q water in the dark at 4 °C (Fisher regenerated cellulose 6000–8000 MW cutoff dialysis membrane) prior to ICP-MS analysis. Platinum-modified plasmid was analyzed by electrophoresis on 1% agarose gels (60 V, 4 °C for 4 h, TAE buffer, pH 7.5). Gels were stained with ethidium bromide (1 μg/mL) for 30 min and washed with water (3 × 100 mL for 15 min). The bands on the gels were visualized and quantified on a Chemidoc XRS imaging system running Quantity One software (Biorad, Hercules, CA). The r_b(c) for each compound was determined by plotting integrated band densities of the relaxed DNA (form 2) vs r_b, and the data was fitted using a quadratic polynomial in SigmaPlot 12.0. Unwinding angles (ϕ) were calculated using the following equation:

$$\phi = 18\sigma/r_b(c)$$

where σ is the superhelical density of the plasmid under the specific conditions of this assay (−0.050, determined by electrophoresis using ethidium bromide with a known unwinding angle of 26°).[35] The r_b(c) values determined for each agent, and the corresponding unwinding angles are means ± standard deviations of three independent experiments.

Cytotoxicity Studies. Cell proliferation assays were carried out using the Celltiter 96 aqueous nonradioactive cell proliferation assay (Promega, Madison, WI). For this assay, all cells were kept in a humidified atmosphere of 5% CO_2 at 37 °C. Cells were seeded into 96-well plates with a total of 740 cells/well for NCI-H460, 10000 cells/well for OCVAR-3, MCF-7, and MDA-MB-231, and 2000 cells/well for PANC-1. Ten mM stock solutions of the tested agents were prepared in DMF and stored at −20 °C. Cells growing in log phase were incubated for 72 h with appropriate serial dilutions of the drugs (starting at a drug concentration of 100 μM). To each well were added 20 μL of MTS/PMS solution, and the mixtures were allowed to equilibrate for 2−4 h. The absorbance of formazan that was produced by bioreduction of MTS was measured at 490 nm (none of the derivatives tested absorbs at this wavelength), and the IC_{50} data was calculated from nonlinear curve fits using a sigmoidal dose−response equation in GraphPad Prism (La Jolla, CA). The calculated IC_{50} values are averages of three individual experiments performed in triplicate.

■ ASSOCIATED CONTENT

Supporting Information

Spectroscopic and analytical data for target compounds, details of the LC-ESMS analysis of reaction mixtures. This material is available free of charge via the Internet at http://pubs.acs.org.

■ AUTHOR INFORMATION

Corresponding Author

*Phone: 336-758-3507. Fax: 336-758-4656. E-mail: bierbau@wfu.edu.

Notes

The authors declare no competing financial interest.

■ ACKNOWLEDGMENTS

This research was sponsored by the National Institutes of Health/National Cancer Institute (grant CA101880). We thank Drs. K. E. Levine and A. S. Essader (RTI International, Research Triangle Park, North Carolina, USA) for the ICP-MS measurements.

■ ABBREVIATIONS USED

ACRAMTU, 1-[2-(acridin-9-ylamino)ethyl]-1,3-dimethylthiourea; ESMS, electrospray mass spectrometry; GMP, guanosine monophosphate; GSH, glutathione; NER, nucleotide excision repair; NSCLC, nonsmall cell lung cancer; r_b, bound platinum-to-nucleotide ratio; r_i, platinum-to-nucleotide incubation ratio

■ REFERENCES

(1) Kelland, L. The resurgence of platinum-based cancer chemotherapy. *Nature Rev. Cancer* **2007**, *7*, 573−784.

(2) Koberle, B.; Tomicic, M. T.; Usanova, S.; Kaina, B. Cisplatin resistance: preclinical findings and clinical implications. *Biochim. Biophys. Acta* **2010**, *1806*, 172−182.

(3) Einhorn, L. H. Testicular cancer: an oncological success story. *Clin. Cancer Res.* **1997**, *3*, 2630−2632.

(4) Archer, V. R.; Billingham, L. J.; Cullen, M. H. Palliative chemotherapy: no longer a contradiction in terms. *Oncologist* **1999**, *4*, 470−477.

(5) Fujii, T.; Toyooka, S.; Ichimura, K.; Fujiwara, Y.; Hotta, K.; Soh, J.; Suehisa, H.; Kobayashi, N.; Aoe, M.; Yoshino, T.; Kiura, K. Date, H. ERCC1 protein expression predicts the response of cisplatin-based neoadjuvant chemotherapy in non-small-cell lung cancer. *Lung Cancer* **2008**, *59*, 377−384.

(6) Cobo, M.; Isla, D.; Massuti, B.; Montes, A.; Sanchez, J. M.; Provencio, M.; Vinolas, N.; Paz-Ares, L.; Lopez-Vivanco, G.; Munoz, M. A.; Felip, E.; Alberola, V.; Camps, C.; Domine, M.; Sanchez, J. J.; Sanchez-Ronco, M.; Danenberg, K.; Taron, M.; Gandara, D.; Rosell, R. Customizing cisplatin based on quantitative excision repair cross-complementing 1 mRNA expression: a phase III trial in non-small-cell lung cancer. *J. Clin. Oncol.* **2007**, *25*, 2747−2754.

(7) Oliver, T. G.; Mercer, K. L.; Sayles, L. C.; Burke, J. R.; Mendus, D.; Lovejoy, K. S.; Cheng, M. H.; Subramanian, A.; Mu, D.; Powers, S.; Crowley, D.; Bronson, R. T.; Whittaker, C. A.; Bhutkar, A.; Lippard, S. J.; Golub, T.; Thomale, J.; Jacks, T.; Sweet-Cordero, E. A. Chronic cisplatin treatment promotes enhanced damage repair and tumor progression in a mouse model of lung cancer. *Genes Dev.* **2010**, *24*, 837−852.

(8) Momekov, G.; Bakalova, A.; Karaivanova, M. Novel approaches towards development of non-classical platinum-based antineoplastic agents: design of platinum complexes characterized by an alternative DNA-binding pattern and/or tumor-targeted cytotoxicity. *Curr. Med. Chem.* **2005**, *12*, 2177−2191.

(9) Komeda, S. Unique platinum−DNA interactions may lead to more effective platinum-based antitumor drugs. *Metallomics* **2011**, *3*, 650−655.

(10) Guddneppanavar, R.; Bierbach, U. Adenine-N3 in the DNA minor groove—an emerging target for platinum containing anticancer pharmacophores. *Anticancer Agents Med. Chem.* **2007**, *7*, 125−138.

(11) Graham, L. A.; Wilson, G. M.; West, T. K.; Day, C. S.; Kucera, G. L.; Bierbach, U. Unusual Reactivity of a Potent Platinum−Acridine Hybrid Antitumor Agent. *ACS Med. Chem. Lett.* **2011**, *2*, 687−691.

(12) Ma, Z.; Choudhury, J. R.; Wright, M. W.; Day, C. S.; Saluta, G.; Kucera, G. L.; Bierbach, U. A non-cross-linking platinum−acridine agent with potent activity in non-small-cell lung cancer. *J. Med. Chem.* **2008**, *51*, 7574−7580.

(13) Qiao, X.; Zeitany, A. E.; Wright, M. W.; Essader, A. S.; Levine, K. E.; Kucera, G. L.; Bierbach, U. Analysis of the DNA damage produced by a platinum−acridine antitumor agent and its effects in NCI-H460 lung cancer cells. *Metallomics* **2012**, *4*, 645−652.

(14) Kostrhunova, H.; Malina, J.; Pickard, A. J.; Stepankova, J.; Vojtiskova, M.; Kasparkova, J.; Muchova, T.; Rohlfing, M. L.; Bierbach, U.; Brabec, V. Replacement of a thiourea with an amidine group in a monofunctional platinum−acridine antitumor agent. Effect on DNA interactions, DNA adduct recognition and repair. *Mol. Pharmaceutics* **2011**, *8*, 1941−1954.

(15) Smyre, C. L.; Saluta, G.; Kute, T. E.; Kucera, G. L.; Bierbach, U. Inhibition of DNA Synthesis by a Platinum−Acridine Hybrid Agent Leads to Potent Cell Kill in Non-Small Cell Lung Cancer. *ACS Med. Chem. Lett.* **2011**, *2*, 870−874.

(16) Alley, S. C.; Okeley, N. M.; Senter, P. D. Antibody−drug conjugates: targeted drug delivery for cancer. *Curr. Opin. Chem. Biol.* **2010**, *14*, 529−537.

(17) Ma, Y.; Day, C. S.; Bierbach, U. Synthesis, structure, and reactivity of monofunctional platinum(II) and palladium(II) complexes containing the sterically hindered ligand 6-(methylpyridin-2-yl)acetate. *J. Inorg. Biochem.* **2005**, *99*, 2013−2023.

(18) Manzotti, C.; Pratesi, G.; Menta, E.; Di Domenico, R.; Cavalletti, E.; Fiebig, H. H.; Kelland, L. R.; Farrell, N.; Polizzi, D.; Supino, R.; Pezzoni, G.; Zunino, F. BBR 3464: A novel triplatinum complex, exhibiting a preclinical profile of antitumor efficacy different from cisplatin. *Clin. Cancer Res.* **2000**, *6*, 2626−2634.

(19) Zhu, L.; Kostic, N. M. Toward artificial metalloproteases: mechanisms by which platinum(II) and palladium(II) complexes promote selective, fast hydrolysis of unactivated amide bonds in peptides. *Inorg. Chem.* **1992**, *31*, 3994−4001.

(20) Wang, X.; Guo, Z. The role of sulfur in platinum anticancer chemotherapy. *Anticancer Agents Med. Chem.* **2007**, *7*, 19−34.

(21) Brabec, V.; Kleinwächter, V.; Butour, J.-L.; Johnson, N. P. Biophysical studies of the modification of DNA by antitumor platinum coordination-complexes. *Biophys. Chem.* **1990**, *35*, 129−141.

(22) Baruah, H.; Rector, C. L.; Monnier, S. M.; Bierbach, U. Mechanism of action of non-cisplatin type DNA-targeted platinum anticancer agents: DNA interactions of novel acridinylthioureas and their platinum conjugates. *Biochem. Pharmacol.* **2002**, *64*, 191−200.

(23) Choudhury, J. R.; Bierbach, U. Characterization of the bisintercalative DNA binding mode of a bifunctional platinum−acridine agent. *Nucleic Acids Res.* **2005**, *33*, 5622−5632.
(24) Choudhury, J. R.; Rao, L.; Bierbach, U. Rates of intercalator-driven platination of DNA determined by a restriction enzyme cleavage inhibition assay. *J. Biol. Inorg. Chem.* **2011**, *16*, 373−380.
(25) Baskin, J. M.; Prescher, J. A.; Laughlin, S. T.; Agard, N. J.; Chang, P. V.; Miller, I. A.; Lo, A.; Codelli, J. A.; Bertozzi, C. R. Copper-free click chemistry for dynamic in vivo imaging. *Proc. Natl. Acad. Sci. U.S.A.* **2007**, *104*, 16793−16797.
(26) Godwin, A. K.; Meister, A.; O'Dwyer, P. J.; Huang, C. S.; Hamilton, T. C.; Anderson, M. E. High resistance to cisplatin in human ovarian cancer cell lines is associated with marked increase of glutathione synthesis. *Proc. Natl. Acad. Sci. U.S.A.* **1992**, *89*, 3070−3074.
(27) Yde, C. W.; Issinger, O. G. Enhancing cisplatin sensitivity in MCF-7 human breast cancer cells by down-regulation of Bcl-2 and cyclin D1. *Int. J. Oncol.* **2006**, *29*, 1397−1404.
(28) Rejiba, S.; Bigand, C.; Parmentier, C.; Hajri, A. Gemcitabine-based chemogene therapy for pancreatic cancer using Ad-dCK::UMK GDEPT and TS/RR siRNA strategies. *Neoplasia* **2009**, *11*, 637−650.
(29) Morgan, M. A.; Parsels, L. A.; Parsels, J. D.; Mesiwala, A. K.; Maybaum, J.; Lawrence, T. S. Role of checkpoint kinase 1 in preventing premature mitosis in response to gemcitabine. *Cancer Res.* **2005**, *65*, 6835−6842.
(30) Wang, R. E.; Costanza, F.; Niu, Y.; Wu, H.; Hu, Y.; Hang, W.; Sun, Y.; Cai, J. Development of self-immolative dendrimers for drug delivery and sensing. *J. Controlled Release* **2012**, *159*, 154−163.
(31) Gelasco, A.; Lippard, S. J. Anticancer activity of cisplatin and related complexes. In *Topics in Biological Inorganic Chemistry*; Clarke, M. J., Sadler, P. J., Eds.; Springer: New York, 1999; pp 1−43.
(32) Dhara, S. C. A rapid method for the synthesis of *cis*-$[Pt(NH_3)_2Cl_2]$. *Indian J. Chem.* **1970**, *8*, 193−194.
(33) Augustus, T. M.; Anderson, J.; Hess, S. M.; Bierbach, U. Bis(acridinylthiourea)platinum(II) complexes: synthesis, DNA affinity, and biological activity in glioblastoma cells. *Bioorg. Med. Chem. Lett.* **2003**, *13*, 855−858.
(34) Martins, E. T.; Baruah, H.; Kramarczyk, J.; Saluta, G.; Day, C. S.; Kucera, G. L.; Bierbach, U. Design, synthesis, and biological activity of a novel non-cisplatin-type platinum−acridine pharmacophore. *J. Med. Chem.* **2001**, *44*, 4492−4496.
(35) DeLeys, R. J.; Jackson, D. A. Electrophoretic analysis of covalently closed SV40 DNA: Boltzmann distributions of DNA species. *Nucleic Acids Res.* **1976**, *3*, 641−652.